The 2010 IEEE/RSJ International Conference on
Intelligent Robots and Systems
October 18-22, 2010, Taipei, Taiwan

Passivity-based Controllers for Periodic Motions of Multi-joint Robots with Impact Phenomena

Mitsunori Uemura and Sadao Kawamura
Department of Robotics, Ritsumeikan University

***Abstract*— This paper proposes passivity-based controllers for periodic motions of multi-joint robots with impact phenomena. Even the robot motions with impact phenomena have complex dynamics, we try to analyze stability of the controlled systems by adopting some assumptions and using Lyapunov-like functions. At first, we present a passivity-based feedback controller. Secondly, we present a repetitive controller based on passivity-based iterative learning control. These controllers generate desired periodic motions, which are specified by users of the controllers. Advantages of the proposed controllers are to works well without using exact parameter values of the controlled systems nor huge numerical calculations.**

***Index Terms*— Impact Phenomenon, Collision, Multi-Joint Robot, Passivity-based Control, Stability Analysis, Lyapunov Function**

I. INTRODUCTION

Robots are expected to perform various tasks depending on demands of their users. Then, various kinds of motions are required to perform such tasks. Periodic motions with impact phenomena are typical motions for the tasks, such as walking and hammering. However, to construct effective control methods is not easy, because of not only nonlinearity of robot dynamics but also discrete dynamics of the impact phenomena. This kind of controlled system are called "hybrid systems", and stability analyses become much more difficult than linear systems without impact phenomena.

To overcome this difficulty, researchers have tried to propose controllers and to analyze stability [1], [2], [3]. Y. Shoji *et al.* proposed a feedback controller for robotic manipulators, which collide with walls [1]. Stability of the controlled systems is proved mathematically. In this case, the proposed controller aims at set point control. J. W. Grizzle *et al.* proposed an controller for underactuated walking robots [2]. The proposed controller guarantees asymptotic stability, and requires parameter values of the robots and numerical calculations of dynamics of the robots.

On the other hand, passivity-based control has been established so as to control robotic systems [4]. Even the robotic systems have nonlinear dynamics, passivity-based controllers achieve control objectives, because these controllers effectively utilize characteristics of energy of the robotic systems. The effective utilization brings about some advantages of the passivity-based controllers. The advantages are to guarantee stability of the controlled systems and to work well without using exact parameter values of the controlled systems nor huge numerical calculations. We also have proposed resonance-based control for robotic systems [5], [6], [7], [8], [9]. The resonance-based controllers realize not only trajectory tracking of periodic motions but also minimization of actuator torque by adjusting stiffness of mechanical elastic elements installed in each joint of the robots. Control strategies of the resonance-based controllers are similar to the passivity-based controllers, and the resonance-based controllers have the same advantages as the passivity-based controllers. However, as far as the authors know, there are no existing controllers, which guarantee stability and does not require precise information of the robotic systems, in the case of periodic motions with impact phenomena. Therefore, to extend passivity-based control to periodic motions with impact phenomena can contribute control theories of robotic systems.

M. W. Spong *et al.* proposed a passivity-based controller for bipedal robots [3]. The proposed controller effectively utilizes the characteristics of energy of the bipedal robots. However, in this case, the proposed controller requires parameter values of the robots and some online numerical calculations of kinetic and potential energy of the robots,

Therefore, this paper tries to extend passivity-based control to the robot motions with impact phenomena, and we design controllers that work without using exact parameter values nor huge numerical calculations. At first, we design a passivity-based feedback controller. This controller is composed of feedback input of an error between a desired motion and an actual motion. Secondly, we design a repetitive controller using the framework of passivity-based iterative learning control. This controller is composed of the error feedback input and a feedfoward input of iterative learning control. These controllers aim at generating desired motions specified by users of the controllers. This paper analyzes stability of the controlled systems. For this purpose, we design the desired motions and adopt some assumptions. Numerical simulations demonstrate the effectiveness of the proposed controllers.

II. PROBLEM FORMULATION

This section formulates a problem of periodic motions of multi-joint robots with impact phenomena as shown in **Fig.1**.

A. Kinematics

Kinematic relationship between a tip position of the multi-joint robots in the Cartesian coordinate $\boldsymbol{x}(t) \in \Re^n$ and joint anlge $\boldsymbol{q}(t) = (q_1 \cdots q_n)^T \in \Re^n$ is described by a nonlinear function $\boldsymbol{f}(\boldsymbol{q}) \in \Re^n$.

$$\boldsymbol{x} = \boldsymbol{f}(\boldsymbol{q}) \tag{1}$$

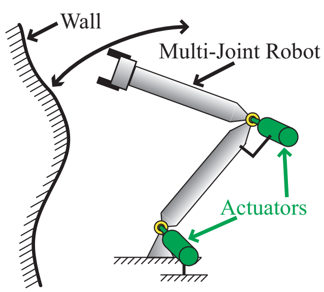

Fig. 1. Robot Motion with Impact Phenomenon

where $n \in \boldsymbol{N}$ is the number of the robot joints. By differentiating the both side of the equation (1), we obtain

$$\dot{\boldsymbol{x}} = \boldsymbol{J}(\boldsymbol{q})\dot{\boldsymbol{q}} \quad (2)$$

where $\boldsymbol{J}(\boldsymbol{q}) \in \Re^{n\times n}$ is a Jacobian matrix between the two coordinate systems $\boldsymbol{x}, \boldsymbol{q}$.

B. Dynamics

Dynamics of the multi-joint robots without considering impact phenomena is given by

$$\boldsymbol{R}(\boldsymbol{q})\ddot{\boldsymbol{q}} + \left\{\frac{1}{2}\dot{\boldsymbol{R}}(\boldsymbol{q}) + \boldsymbol{S}(\boldsymbol{q},\dot{\boldsymbol{q}}) + \boldsymbol{D}\right\}\dot{\boldsymbol{q}} + \boldsymbol{g}(\boldsymbol{q}) = \boldsymbol{\tau}, \quad (3)$$

where $\boldsymbol{R}(\boldsymbol{q}) \in \Re^{n\times n}$ is a positive definite inertia matrix, $\boldsymbol{S}(\boldsymbol{q},\dot{\boldsymbol{q}}) \in \Re^{n\times n}$ is a skew symmetric matrix, $\boldsymbol{D} = \mathrm{diag}(d_1 \cdots d_n) \in \Re^{n\times n}$ is a viscosity matrix, $\boldsymbol{g}(\boldsymbol{q}) \in \Re^n$ is a vector of gravitational torque, and $\boldsymbol{\tau} = (\tau_1 \cdots \tau_n)^T$ is a vector of actuator torque.

C. Impact Phenomena

When a tip of the robot collides with a wall, impact phenomenon will occur. As a first step to establish the passivity-based control theory considering the impact phenomena, this paper adopts a simple model of the impact phenomena, and we assume that impact phenomena occur instantly. At the instant, the tip of the robot is on the surface of the wall, and the tip position $\boldsymbol{x}$ satisfies

$$f_{wall}(\boldsymbol{x}(t_{si})) = 0, \quad (4)$$

where $f_{wall} \in \Re$ describes the surface of the wall, and t_{si} is the time of $i \in \boldsymbol{N}$th impact.

Since the impact phenomena are assumed to occur instantly, the joint angle $\boldsymbol{q}$ does not change at the impact phenomena.

$$\boldsymbol{q}(t_{si}^+) = \boldsymbol{q}(t_{si}^-) = \boldsymbol{q}(t_{si}) \quad (5)$$

where $t_{si}^+ \in \Re$ is the time just after the impact, and $t_{si}^- \in \Re$ is the time just before the impact.

To the contrary, the joint velocity $\dot{\boldsymbol{q}}$ changes at the impact.

$$\dot{\boldsymbol{q}}(t_{si}^+) = \boldsymbol{\Phi}(\boldsymbol{q}(t_{si}^-))\dot{\boldsymbol{q}}(t_{si}^-) \quad (6)$$

where $\boldsymbol{\Phi} \in \Re^{n\times n}$ is a matrix that represents the velocity change at the impact instants [2].

Since the wall is passive, the wall does not supply energy to the robot. Therefore, kinetic energy of the robots will be reduced or conserved at the impact.

$$\frac{1}{2}\dot{\boldsymbol{q}}(t_{si}^+)^T\boldsymbol{R}\dot{\boldsymbol{q}}(t_{si}^+) = \frac{1}{2}\dot{\boldsymbol{q}}(t_{si}^-)^T\boldsymbol{\Phi}^T\boldsymbol{R}\boldsymbol{\Phi}\dot{\boldsymbol{q}}(t_{si}^-)$$
$$\leq \frac{1}{2}\dot{\boldsymbol{q}}(t_{si}^-)^T\boldsymbol{R}(\boldsymbol{q})\dot{\boldsymbol{q}}(t_{si}^-) \quad (7)$$

D. Control Objective

A control objective of passivity-based controllers in this study is to generate desired periodic motion $\boldsymbol{q} \to \boldsymbol{q_d} \in \Re^n$. The periodic motion includes a impact phenomenon in a cycle.

E. Design of Desired Motion

Here, we design the desired motion $\boldsymbol{q_d}$. As stated in the control objective, the actual motion $\boldsymbol{q}$ is controlled to be periodic with a desired cycle time $T_d \in \Re$. However, actual cycle time $T_i = t_{si} - t_{s(i-1)} \in \Re$ of the ith cycle can be different from the desired one $T_i \neq T_d$ due to tracking errors. Therefore, the desired motion $\boldsymbol{q_d}(t)$ of ith cycle is designed by using a reference motion $\boldsymbol{q_r} \in \Re^n$

$$\boldsymbol{q_d}(t) = \boldsymbol{q_r}(t - t_{s(i-1)}). \quad (8)$$

The reference motion $\boldsymbol{q_r}$ represents a cycle of the desired motion. The reference motion $\boldsymbol{q_r}$ is designed in the certain period $\boldsymbol{q_r}(t)$ $(0 \leq t \leq T_d + T_s)$ so that the actual cycle time T_i will converge to the desired one T_d if the actual motion converge to the desired one $\boldsymbol{q} \to \boldsymbol{q_d}$, where $T_s \in \Re$ is a positive constant. The reference motion $\boldsymbol{q_r} \in \Re^n$ should be continuous

$$|\boldsymbol{q_r}| \leq c_{bp}, \quad |\dot{\boldsymbol{q}}_{\boldsymbol{r}}| \leq c_{bs}, \quad |\ddot{\boldsymbol{q}}_{\boldsymbol{r}}| \leq c_{ba}, \quad (9)$$

where $c_{bp}, c_{bs}, c_{ba} \in \Re$ are positive constants. Since the tip of the robot is on the surface of the wall at the instants of the impact phenomena, $\boldsymbol{q_r}(0)$ and $\boldsymbol{q_r}(T_d)$ are designed to satisfy

$$\boldsymbol{q_r}(0) = \boldsymbol{q_r}(T_d) \quad (10)$$
$$f_{wall}(\boldsymbol{f}(\boldsymbol{q_r}(0))) = f_{wall}(\boldsymbol{f}(\boldsymbol{q_r}(T_d))) = 0 \quad (11)$$

In other periods $(0 < t < T_d,\ T_d < t \leq T_d + T_s)$, $\boldsymbol{q_r}(t)$ is not always on the surface of the wall $f_{wall}(\boldsymbol{q_r}(t)) \neq 0$. The initial velocity $\boldsymbol{q_r}(0)$ is designed with considering the impact phenomena of the equation (6),

$$\dot{\boldsymbol{q}}_{\boldsymbol{r}}(0) = \hat{\boldsymbol{\Phi}}\dot{\boldsymbol{q}}_{\boldsymbol{r}}(T_d) \quad (12)$$

where $\hat{\boldsymbol{\Phi}} \in \Re^{n\times n}$ is an estimated matrix of $\boldsymbol{\Phi}(\boldsymbol{q_r}(T_d))$.

To guarantee stability of the controlled system, we introduce some conditions for the desired motion. The first condition relates to a distance between the reference motion $\boldsymbol{q_r}$ and the wall. This condition is defined so that the largest value of $c_w = \frac{||\boldsymbol{q_r}(T_d) - \boldsymbol{q_f}||}{||\boldsymbol{q_r}(t) - \boldsymbol{q_f}||}$ in the certain period $T_d - T_s < t < T_d + T_s$ is smaller than a certain positive constant $c_w \leq c_{wmax}$ as shown in **Fig.2** for all $\boldsymbol{q_f}$, where $\boldsymbol{q_f} \in \Re^n$ is a vector that satisfies $f_{wall}(\boldsymbol{f}(\boldsymbol{q_f})) = 0$. This kind of vector norm $||\boldsymbol{q_r}(t) - \boldsymbol{q_f}||$ is defined as $||\boldsymbol{q_r}(t) - \boldsymbol{q_f}|| = (\boldsymbol{q_r}(t) - \boldsymbol{q_f})^T(\boldsymbol{q_r}(t) - \boldsymbol{q_f})$. Therefore, we obtain the following inequality for all $\boldsymbol{q_f}$.

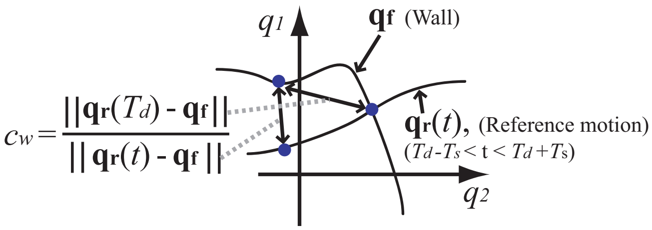

Fig. 2. Distance between Reference Motion and Wall

$$||\boldsymbol{q_r}(T_d) - \boldsymbol{q_f}|| \leq c_{wmax}||\boldsymbol{q_r}(t) - \boldsymbol{q_f}|| \tag{13}$$

The second condition relates to a velocity profile. This condition is defined in the certain period $T_d - T_s < t < T_d + T_s$ as

$$||\dot{\boldsymbol{q}}_{\boldsymbol{r}}(t) - \dot{\boldsymbol{q}}_{\boldsymbol{r}}(T_d)|| \leq c_v||\boldsymbol{q_r}(t) - \boldsymbol{q_r}(T_d)|| \tag{14}$$

Therefore, the reference motion is designed so as not to have large velocity change around the time T_d. For example, if the reference motion is a constant acceleration motion $q_{ri}(t) = c_a t^2 + c_s t + c_p$ $(i = 1, 2, 3 \cdots)$, we can set the coefficient c_v of the equation (14) to $c_v = \frac{2c_a}{c_s}$, where $c_a, c_s, c_p \in \Re$ are positive constants.

The above design of the desired motion requires some information of the wall surfaces. The equation (11) requires information of a position of the surface at a point. To guarantee small c_{wmax} require rough information of shape of the surface in some region.

However, to obtain the above information seems not so difficult, because the impact position $\boldsymbol{q_r}(0), \boldsymbol{q_r}(T_d)$ can be obtained by some trial movements of the robots or some sensors, such as laser rangefinders. In addition, the rough information of the wall shape for the first condition can be also obtained by some laser rangefinders or cameras.

F. Assumption

In order to discuss stability, we introduce some assumptions of the kinematics and the dynamics. The first assumption is that the kinematics of the robots $\boldsymbol{f}(\boldsymbol{q})$ satisfies the following Lipschitz condition for all $\boldsymbol{q_1}, \boldsymbol{q_2} \in \Re^n$.

$$||\boldsymbol{f}(\boldsymbol{q_1}) - \boldsymbol{f}(\boldsymbol{q_2})|| \leq L_1||\boldsymbol{q_1} - \boldsymbol{q_2}||, \tag{15}$$

where $L_1 \in \Re$ is a positive constant. Kinematics of usual robots satisfies this assumption.

The second assumption is that the robot does not move around neighborhood of singular positions. Then, the Jacobian matrix becomes always full-rank, and the following Lipschitz condition is satisfied for all $\boldsymbol{q_1}, \boldsymbol{q_2}$

$$||\boldsymbol{q_1} - \boldsymbol{q_2}|| \leq L_2||\boldsymbol{f}(\boldsymbol{q_1}) - \boldsymbol{f}(\boldsymbol{q_2})|| \tag{16}$$

where $L_2 \in \Re$ is a positive constant. Moreover, we assume that impact dynamics also satisfies the following Lipschitz condition for all $\boldsymbol{q_1}, \boldsymbol{q_2}$.

$$||\boldsymbol{\Phi}(\boldsymbol{q_1}) - \boldsymbol{\Phi}(\boldsymbol{q_2})|| \leq L_3||\boldsymbol{q_1} - \boldsymbol{q_2}||, \tag{17}$$

where $L_3 \in \Re$ is a positive constant. If the impact phenomenon is an elastic collision and the equation (16) is satisfied, this assumption seems reasonable.

Next, we assume that initial tracking errors $\boldsymbol{q}(0) - \boldsymbol{q_d}(0), \dot{\boldsymbol{q}}(0) - \dot{\boldsymbol{q}}_{\boldsymbol{d}}(0)$ are finite.

$$||\boldsymbol{q}(0) - \boldsymbol{q_d}(0)|| + ||\dot{\boldsymbol{q}}(0) - \dot{\boldsymbol{q}}_{\boldsymbol{d}}(0)|| < c_e \tag{18}$$

where $c_e \in \Re$ is a positive constant. Namely, the stability that we analyze in this paper is in the sense of not global but local.

The last assumption is that the impact phenomena always occur in a certain period, and the actual cycle time T_i satisfies

$$T_d - T_s < T_i < T_d + T_s. \tag{19}$$

When the motion is controlled precisely by feedback controllers to some extent, the assumption of the equation (19) seems not so unreasonable.

III. Passivity-based Feedback Control

A. Controller Design

To generate the desired motion $\boldsymbol{q} \to \boldsymbol{q_d}$, we propose the following passivity-based feedback controller.

$$\boldsymbol{\tau} = -\boldsymbol{K_v}\Delta\dot{\boldsymbol{q}} - \boldsymbol{K_p}\Delta\boldsymbol{q} \tag{20}$$

where $\boldsymbol{K_v}, \boldsymbol{K_p} \in \Re^{n\times n}$ are feedback gain matrices, and $\Delta\boldsymbol{q} = \boldsymbol{q} - \boldsymbol{q_d}$.

This controller does not require exact parameter values of the robots nor huge numerical calculations.

B. Stability Analysis

We introduce the following Lyapunov-like function to prove stability of the controlled systems.

$$\begin{aligned} V(t) \;\; = \;\; & \frac{1}{2}\Delta\dot{\boldsymbol{q}}^T\boldsymbol{R}(\boldsymbol{q})\Delta\dot{\boldsymbol{q}} + \frac{1}{2}\Delta\boldsymbol{q}^T(\boldsymbol{K_p} + \alpha\boldsymbol{K_v})\Delta\boldsymbol{q} \\ & + \alpha\Delta\dot{\boldsymbol{q}}^T\boldsymbol{R}(\boldsymbol{q})\Delta\boldsymbol{q} \end{aligned} \tag{21}$$

where $\alpha \in \Re$ is a positive constant. The function V becomes positive definite by selecting enough small α, because there are finite positive constants c_{dq}, c_q that satisfy $\Delta\dot{\boldsymbol{q}}^T\boldsymbol{R}(\boldsymbol{q})\Delta\boldsymbol{q} \leq c_{dq}||\Delta\dot{\boldsymbol{q}}|| + c_q||\Delta\boldsymbol{q}||$. Note that α can be larger with increase of the feedback gain $\boldsymbol{K_v}$ [4].

When the robot does not collide with the wall and the conditions of the equations (9), (18) are satisfied, it is proved [12] that time derivative of V is bounded by

$$\begin{aligned} \dot{V}(t) \;\; \leq \;\; & -\Delta\dot{\boldsymbol{q}}^T\left(\boldsymbol{K_v} - c_1\right)\Delta\dot{\boldsymbol{q}} - \alpha\Delta\boldsymbol{q}^T\left(\boldsymbol{K_p} - c_2\right)\Delta\boldsymbol{q} \\ & + c_3 \end{aligned} \tag{22}$$

where $c_1, c_2, c_3 \in \Re$ are positive constants that are independent of feedback gains $\boldsymbol{K_v}, \boldsymbol{K_p}$.

Therefore, if we set enough large feedback gains $\boldsymbol{K_v}, \boldsymbol{K_p}$, $V(t)$ exponentially converges to a certain region $V(t) \leq c_4$ excepting the instants of the impact phenomena. Then, $V(t_{si}^-)$ is bounded by

$$\begin{aligned} V(t_{si}^-) \;\; \leq \;\; & V(t_{s(i-1)}^+) + c_4 \\ & -(1 - e^{-c_5 T_i})\left\{||\Delta\dot{\boldsymbol{q}}(t_{s(i-1)}^+)||_{\frac{1}{2}\boldsymbol{R}(\boldsymbol{q})} \right. \\ & \left. + ||\Delta\boldsymbol{q}(t_{s(i-1)}^+)||_{\frac{1}{2}(\boldsymbol{K_p}+\alpha\boldsymbol{K_v})}\right\}. \end{aligned} \tag{23}$$

where $c_5 \in \Re$ is a positive constant. This kind of vector norm with the suffix $||\Delta\dot{\boldsymbol{q}}(t_{s(i-1)}^+)||_{\frac{1}{2}\boldsymbol{R}(\boldsymbol{q})}$ is defined as $||\Delta\dot{\boldsymbol{q}}(t^+_{s(i-1)})||_{\frac{1}{2}\boldsymbol{R}(\boldsymbol{q})} = \frac{1}{2}\Delta\dot{\boldsymbol{q}}(t^+_{s(i-1)})^T\boldsymbol{R}(\boldsymbol{q})\Delta\dot{\boldsymbol{q}}(t^+_{s(i-1)})$. The value of c_5 can be increased by setting larger feedback gains $\boldsymbol{K_v}, \boldsymbol{K_p}$.

Next, we consider the function V at the impact. Since the equation (13) is satisfied for all $\boldsymbol{q_f}$, the norm of the position error just after the impact $||\Delta\boldsymbol{q}(t^+_{si})||$ can be bounded by the norm just before the impact $c_{wmax}||\Delta\boldsymbol{q}(t^-_{si})||$.

$$\begin{aligned}||\Delta\boldsymbol{q}(t^+_{si})|| &= ||\boldsymbol{q_r}(0) - \boldsymbol{q}(t^+_{si})|| = ||\boldsymbol{q_r}(T_d) - \boldsymbol{q_f}|| \\ &\le c_{wmax}||\boldsymbol{q_r}(T_i) - \boldsymbol{q}(t^-_{si})|| = c_{wmax}||\Delta\boldsymbol{q}(t^-_{si})|| \quad (24)\end{aligned}$$

The norm of the velocity error just after the impact $\Delta\dot{\boldsymbol{q}}(t^+_{si})$ also can be bounded as follows. At first, we rewrite $\Delta\dot{\boldsymbol{q}}(t^+_{si})$ as

$$\begin{aligned}\Delta\dot{\boldsymbol{q}}(t^+_{si}) \;\;=\;\; & \boldsymbol{\Phi}\Delta\dot{\boldsymbol{q}}(t^-_{si}) + \boldsymbol{\Phi}\left\{\dot{\boldsymbol{q}}_{\boldsymbol{d}}(t^-_{si}) - \dot{\boldsymbol{q}}_{\boldsymbol{r}}(T_d)\right\} \\ & + \left\{\boldsymbol{\Phi} - \hat{\boldsymbol{\Phi}}\right\}\dot{\boldsymbol{q}}_{\boldsymbol{r}}(T_d) \quad (25)\end{aligned}$$

If the impact dynamics is known and we can set $\hat{\boldsymbol{\Phi}}$ to $\boldsymbol{\Phi}(\boldsymbol{q_r}(T_d))$, the third term of right-hand side of the equation (25) is bounded by using the equation (13) and (17) as

$$||\left\{\boldsymbol{\Phi}(\boldsymbol{q}(t_{si})) - \hat{\boldsymbol{\Phi}}\right\}\dot{\boldsymbol{q}}_{\boldsymbol{r}}(T_d)|| \le L_3 c_{wmax}||\Delta\boldsymbol{q}(t^-_{si})||, \quad (26)$$

If the impact dynamics is unknown $\hat{\boldsymbol{\Phi}} \ne \boldsymbol{\Phi}(\boldsymbol{q_r}(T_d))$, the term $\left\{\hat{\boldsymbol{\Phi}} - \boldsymbol{\Phi}(\boldsymbol{q}(t_{si})\right\}\dot{\boldsymbol{q}}_{\boldsymbol{r}}(T_d)$ is bounded as

$$\begin{aligned}&||\left\{\hat{\boldsymbol{\Phi}} - \boldsymbol{\Phi}(\boldsymbol{q}(t_{si}))\right\}\dot{\boldsymbol{q}}_{\boldsymbol{r}}(T_d)|| \\ &= ||\left\{\boldsymbol{\Phi}(\boldsymbol{q_r}(T_d)) - \boldsymbol{\Phi}(\boldsymbol{q}(t_{si})) + \hat{\boldsymbol{\Phi}} - \boldsymbol{\Phi}(\boldsymbol{q_r}(T_d))\right\}\dot{\boldsymbol{q}}_{\boldsymbol{r}}(T_d)|| \\ &\le 2L_3 c_{wmax}||\Delta\boldsymbol{q}(t^-_{si})|| + c_6, \quad (27)\end{aligned}$$

where $c_6 \in \Re$ is a positive constant. The value of c_6 increases if the difference between $\hat{\boldsymbol{\Phi}}$ and $\boldsymbol{\Phi}(\boldsymbol{q_r}(T_d))$ is larger.

From the desired motion conditions (13), (14), the second term of the right-hand side of the equation (25) can be rewritten as

$$\begin{aligned}&||\dot{\boldsymbol{q}}_{\boldsymbol{d}}(t^-_{si}) - \dot{\boldsymbol{q}}_{\boldsymbol{r}}(T_d)|| = ||\dot{\boldsymbol{q}}_{\boldsymbol{r}}(t^-_{si} - t_{s(i-1)}) - \dot{\boldsymbol{q}}_{\boldsymbol{r}}(T_d)|| \\ &\le c_v||\boldsymbol{q_r}(t^-_{si} - t_{s(i-1)}) - \boldsymbol{q_r}(T_d)|| \\ &= c_v||\Delta\boldsymbol{q}(t^-_{si}) + \boldsymbol{q}(t^-_{si}) - \boldsymbol{q_r}(T_d)|| \\ &\le 2c_v||\Delta\boldsymbol{q}(t^-_{si})|| + 2c_{wmax}||\boldsymbol{q_f} - \boldsymbol{q_r}(T_d)|| \\ &\le 2c_v(1 + c_{wmax})||\Delta\boldsymbol{q}(t^-_{si})||. \quad (28)\end{aligned}$$

Then, by considering the equation (7), the norm of the velocity error $||\Delta\dot{\boldsymbol{q}}(t^+_{si})||$ is bounded by

$$||\Delta\dot{\boldsymbol{q}}(t^+_{si})|| \le c_7||\Delta\dot{\boldsymbol{q}}(t^-_{si})|| + c_8||\Delta\boldsymbol{q}(t^-_{si})|| + c_9 \quad (29)$$

where $c_7, c_8, c_9 \in \Re$ are positive constants. In the case of $\hat{\boldsymbol{\Phi}} = \boldsymbol{\Phi}(\boldsymbol{q_r}(T_d))$, c_9 becomes 0. Therefore, by using the equation (21), (24), (29), the function V after the impact phenomena is bounded by

$$\begin{aligned}V(t^+_{si}) \;\;\le\;\; & V(t^-_{si}) + c_{10}\left\{||\Delta\dot{\boldsymbol{q}}(t^-_{si})||_{\frac{1}{2}\boldsymbol{R}(\boldsymbol{q})}\right. \\ & \left. + ||\Delta\dot{\boldsymbol{q}}(t^-_{si})||_{\frac{1}{2}(\boldsymbol{K_p} + \alpha\boldsymbol{K_v})}\right\} + c_{11} \quad (30)\end{aligned}$$

where $c_{10}, c_{11} \in \Re$ is a positive constant. The value of c_{10} is independent of the feedback gains $\boldsymbol{K_v}, \boldsymbol{K_p}$, because the equations from (24) to (29) are independent of the feedback gains. The value of c_{11} also becomes 0, in the case of $\hat{\boldsymbol{\Phi}} = \boldsymbol{\Phi}(\boldsymbol{q_r}(T_d))$.

From the equation (23), (30), we obtain

$$V(t^+_{si}) \le c_{12}V(t^+_{s(i-1)}) + c_{13} \quad (31)$$

where $c_{12}, c_{13} \in \Re$ are positive constants. The constant c_{12} decrease if we select large feedback gains $\boldsymbol{K_v}, \boldsymbol{K_p}$, because c_5 will increase by setting larger feedback gains. Therefore, if we set enough large feedback gains $\boldsymbol{K_v}, \boldsymbol{K_p}$, c_{12} can be less than 1.

The equation (31) with $0 < c_{12} < 1$ means that the controlled system is stable, even if the controlled system has the nonlinear dynamics and includes the impact phenomena.

IV. Repetitive Control

The proposed feedback controller in the section III is composed of only the error feedback terms. Therefore, the tracking errors $\Delta\boldsymbol{q}, \Delta\dot{\boldsymbol{q}}$ do not converge to 0. This section proposes a repetitive controller using a feedfoward term based on iterative learning control to realize convergence of the tracking errors to 0.

A. Controller

We use a feedfoward input $\boldsymbol{u}_i(t) \in \Re^n$ of the ith cycle based on iterative learning control for the design of the actuator torque $\boldsymbol{\tau}(t)$.

$$\boldsymbol{\tau}(t) = -\boldsymbol{K_v}\Delta\dot{\boldsymbol{q}} - \boldsymbol{K_p}\Delta\boldsymbol{q} + \boldsymbol{u}_i(t - t_{s(i-1)}). \quad (32)$$

In the cases of usual iterative learning control, a feedfoward input of a cycle is updated by using signals of its previous cycle. However, in this study, the every cycle time T_i can be different from each other, and there can be no corresponding signals of its previous cycle. Therefore, the feedfoward input $\boldsymbol{u}_i$ of the ith cycle ($i \ge 2$) is updated by using signals of the $m(t) \in \boldsymbol{N}$th cycles.

$$\begin{aligned}\boldsymbol{u}_i(t - t_{s(i-1)}) &= \boldsymbol{u}_m(t - t_{s(i-1)}) \\ &\quad -\beta\left\{\Delta\dot{\boldsymbol{q}}(t - t_{pre}(t)) + \alpha\Delta\boldsymbol{q}(t - t_{pre}(t))\right\}, \quad (33)\end{aligned}$$

where $\beta \in \Re$ is a learning gain, and $t_{pre}(t) = \sum_{j=m(t)}^{i-1} T_j$. We adopt the latest cycles ($m(t) < i$) that are longer than the current time from the previous ($i-1$th) impact $t - t_{s(i-1)} \le T_m$ as the $m(t)$th cycles. If there are no latest cycles, $\boldsymbol{u}_i(t - t_{s(i-1)})$ is set to $\boldsymbol{u}_i(t - t_{s(i-1)}) = \boldsymbol{u_0}(t - t_{s(i-1)}) = 0$. For example, as shown in **Fig.3**, when actual cycle times before a 4th cycle are $T_1 = 0.8, T_2 = 1.1, T_3 = 0.9$, we set $m(t)$ of the 4th cycle to $m(t) = 3$ ($t_{s3} < t \le t_{s3} + T_3$), $m(t) = 2$ ($t_{s3} + T_3 < t \le t_{s3} + T_2$), $u_4(t - t_{s3}) = 0$ ($t_{s3} + T_2 < t$).

The proposed controller in this section also does not require exact parameter values of the robots nor huge numerical calculations.

B. Stability Analysis

S. Nakada *et al.* introduced a kind of Lyapunov function that includes an integral term of an error of a feedfoward input [11]. We utilize this technique and define the following Lyapunov-like function $V_2(t)$ of ith cycles ($t_{s(i-1)} < t < t_{si}$) using the function $V(t)$ of the equation (21).

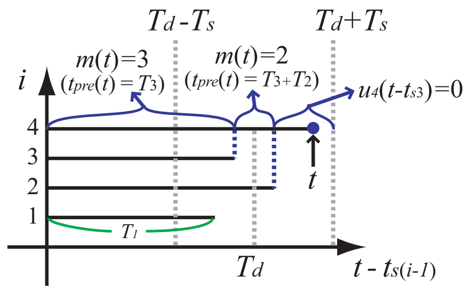

Fig. 3. Definition of mth Cycle

$$V_2(t) = V(t) + \frac{1}{2\beta}\int_t^{t+T_i} ||\Delta \boldsymbol{u}_p(t - t_{s(p-1)})||\mathrm{d}t + \frac{1}{2\beta}\int_{t_{si}}^{t_{s(i-1)}+T_d+T_s} ||\Delta \boldsymbol{u}_p(t - t_{s(p-1)})||\mathrm{d}t, \quad (34)$$

where $\Delta \boldsymbol{u}_p(t) \in \Re^n$ is an error of the feedfoward input $\Delta \boldsymbol{u}_p(t) = \boldsymbol{u}_p(t) - \boldsymbol{u_d}(t)$, $\boldsymbol{u_d}(t) \in \Re^n$ is a necessary torque to generate the desired motion $\boldsymbol{u_d} = \boldsymbol{R}(\boldsymbol{q_d})\ddot{\boldsymbol{q}}_{\boldsymbol{d}} + \left\{\frac{1}{2}\dot{\boldsymbol{R}}(\boldsymbol{q_d}) + \boldsymbol{S}(\boldsymbol{q_d}, \dot{\boldsymbol{q}}_{\boldsymbol{d}}) + \boldsymbol{D}\right\}\dot{\boldsymbol{q}}_{\boldsymbol{d}} + \boldsymbol{g}(\boldsymbol{q_d})$, and $p(t) \in \boldsymbol{N}$ is a positive integer. We adopt the earliest cycles that are longer than the time t from the previous ($i-1$th) impact $t - t_{s(i-1)} \leq T_p$ as the $p(t)$th cycles. If there is no earliest cycles, $p(t)$ is set to 0. For the example of the section IV-A, therefore, $p(t)$ of the 1st cycle is $p(t) = 1$ $(0 < t < T_1)$, $p(t) = 2$ $(T_1 < t < T_2)$, $p(t) = 0$ $(T_2 < t)$. Then, the sum of the integral terms of the equation (34) is continuous with respect to t.

Time derivative of $V_2(t)$ becomes

$$\dot{V}_2(t) \leq -\Delta\dot{\boldsymbol{q}}^T(\boldsymbol{K_v} - c_{13} - \beta)\Delta\dot{\boldsymbol{q}} - \Delta\boldsymbol{q}^T\left(\alpha\boldsymbol{K_p} - c_{14} - \beta\alpha^2\right)\Delta\boldsymbol{q} \quad (35)$$

where $c_{13}, c_{14} \in \Re$ are positive constants, which are independent of the feedback gains $\boldsymbol{K_v}, \boldsymbol{K_p}$. Therefore, by setting enough large feedback gains $\boldsymbol{K_v}, \boldsymbol{K_p}$ and enough small values of α, β, the function $V_2(t)$ monotonically decreases except the instants of the impact phenomena.

Since the integral terms of $V_2(t)$ does not change at the impact phenomena, the same discussion as the equations from (24) to (30) can be applied to V_2. Therefore, in the case of $\hat{\boldsymbol{\Phi}} = \boldsymbol{\Phi}(\boldsymbol{q_r}(T_d))$, we obtain

$$V_2(t_{si}^+) \leq V_2(t_{si}^-) + c_{10}\left\{||\Delta\dot{\boldsymbol{q}}(t_{si}^-)||_{\frac{1}{2}\boldsymbol{R}(\boldsymbol{q})} + ||\Delta\dot{\boldsymbol{q}}(t_{si}^-)||_{\frac{1}{2}(\boldsymbol{K_p}+\alpha\boldsymbol{K_v})}\right\} \quad (36)$$

Then, by integrating the equation (35) by t with considering the equation (36), we obtain

$$V_2(t) - V_2(0) \leq -\int_0^t \left\{||\Delta\dot{\boldsymbol{q}}(t)||_{\boldsymbol{K_v}-c_{13}} + ||\Delta\boldsymbol{q}(t)||_{\alpha\boldsymbol{K_p}-c_{14}}\right\}\mathrm{d}t + \sum_{j=1}^{i-1} c_{10}\left\{||\Delta\dot{\boldsymbol{q}}(t_{sj}^-)||_{\frac{1}{2}\boldsymbol{R}(\boldsymbol{q})} + ||\Delta\boldsymbol{q}(t_{sj}^-)||_{\frac{1}{2}(\boldsymbol{K_p}+\alpha\boldsymbol{K_v})}\right\}. \quad (37)$$

If we set large feedback gains $\boldsymbol{K_v}, \boldsymbol{K_p}$, we can expect that the following inequality is satisfied in the enery ith cycle, because increase ratio of left-hand side of the equation (38) with respect to the feedback gains is higher than the right-hand side.

$$\int_{t_{s(i-1)}^+}^{t_{si}^-} \left\{||\Delta\dot{\boldsymbol{q}}(t)||_{\boldsymbol{K_v}-c_{13}} + ||\Delta\boldsymbol{q}(t)||_{\alpha\boldsymbol{K_p}-c_{14}}\right\}\mathrm{d}t > c_{10}\left\{||\Delta\dot{\boldsymbol{q}}(t_{si}^-)||_{\frac{1}{2}\boldsymbol{R}(\boldsymbol{q})} + ||\Delta\boldsymbol{q}(t_{si}^-)||_{\frac{1}{2}(\boldsymbol{K_p}+\alpha\boldsymbol{K_v})}\right\} \quad (38)$$

Then, $V_2(t)$ decreases at the every cycle, will converge to a constant, and the tracking errors $||\Delta\dot{\boldsymbol{q}}(t)||, ||\Delta\boldsymbol{q}(t)||$ will converge to zero.

Therefore, the proposed repetitive controller in this section can realize trajectory tracking. However, the discussed stability is not mathematically rigorous, because we introduced the assumption of the equation (38). Even to assume the equation (38) is reasonable in the case of large feedback gains, to prove more rigorous stability is our important future work.

V. Simulation

We conducted a numerical simulation to verify the effectiveness of the proposed controller.

A. Condition

We used a two joint robot arm model as shown in **Fig.4** for the simulation. Physical parameters of the robot were set as follows. Mass of the first link was $m_1 = 3.0$[kg], and mass of the second link was $m_2 = 2.0$[kg]. Length of the each link was $l_1 = 0.3$[m], $l_2 = 0.25$[m]. Length from the each joint to the each mass center of the link was $l_{g1} = 0.13$[m], $l_{g2} = 0.1$[m]. Inertia moment of the each link was $I_1 = 0.01$[Nms^2/rad], $I_2 = 0.005$[Nms^2/rad].

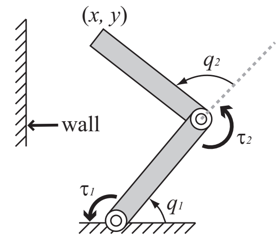

Fig. 4. Simulation Model

The tip position of the robot was described by $\boldsymbol{x} = \begin{pmatrix} x \\ y \end{pmatrix} = \begin{pmatrix} l_1\cos q_1 + l_2\cos(q_1+q_2) \\ l_1\sin q_1 + l_2\sin(q_1+q_2) \end{pmatrix}$[m]. The surface of the wall was described by $f_{wall}(\boldsymbol{x}) = x + 0.2 = 0$[m]. The impact phenomena were assumed to be elastic collisions with a reflection coefficient 0.5.

The repetitive controller of the equations (32), (33) was adopted as the controller. In the stability analysis of the section IV, we need many conditions to guarantee the stability, because the stability analysis becomes conservative due to handling the nonlinearity of the dynamics and the discrete dynamics of the impact phenomena. However, these conditions may not be so severe actually. Therefore, in this simulation, we selected some conditions that may threaten the stability conditions. Namely, the feedback gains $\boldsymbol{K_v}, \boldsymbol{K_p}$ were set to small values $k_{v1} = 5.0, k_{v2} = 2.0$[Nms/rad], $k_{p1} = 25.0, k_{p2} = 4.0$[Nm/rad], the initial tracking errors were set to large $\Delta q_1 = \Delta q_2 = 0.2\pi$[rad], $\Delta\dot{q}_1 = \pi, \Delta\dot{q}_2 =$

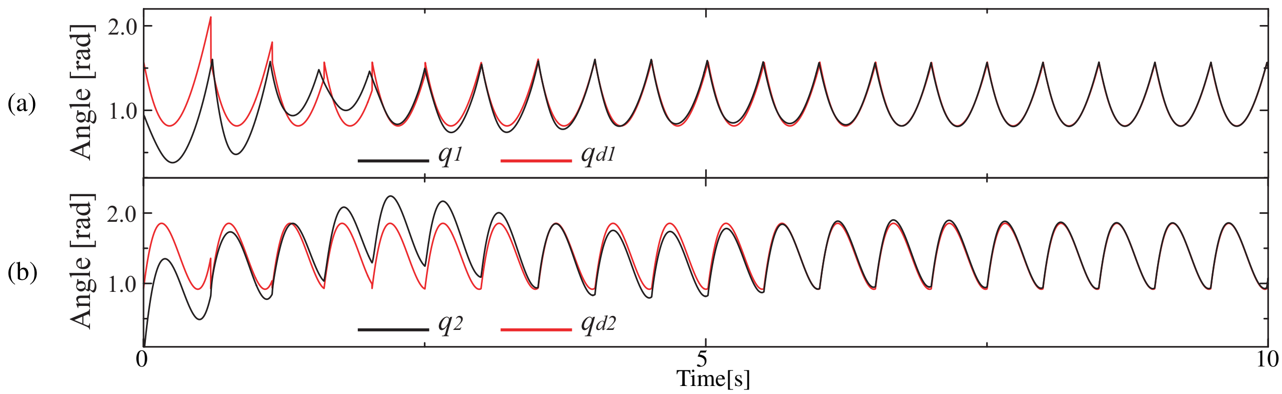

Fig. 5. Simulation Results of Joint Angles

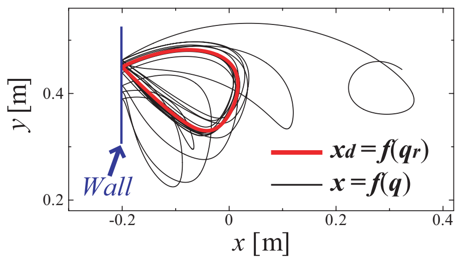

Fig. 6. Tip Position

2.0π[rad/s]. Other gains were selected as $\beta = 1.0$, $\alpha = 5.0$. The reference motion was designed using cubic functions of t so that some conditions of the desired motion was satisfied $f_{wall}(\boldsymbol{f}(\boldsymbol{q_r}(0))) = f_{wall}(\boldsymbol{f}(\boldsymbol{q_r}(T))) = 0, \dot{\boldsymbol{q}}_{\boldsymbol{r}}(0) = \hat{\boldsymbol{\Phi}}\dot{\boldsymbol{q}}_{\boldsymbol{r}}(T)$. The tip trajectory of the reference motion $\boldsymbol{x_d} = \boldsymbol{f}(\boldsymbol{q_r})$ and the wall is shown in **Fig.6**. The desired motion may be like a hammering motion. The estimated matrix $\hat{\boldsymbol{\Phi}}$ was set to the actual one $\boldsymbol{\Phi}(\boldsymbol{q_r}(T_d))$.

B. Result

Simulation results are shown in **Fig.5**, Fig.6, and **an accompanying video**. Since we selected large initial tracking errors $\Delta\boldsymbol{q}(0), \Delta\dot{\boldsymbol{q}}(0)$ and small feedback gains, tracking errors were large during the first 5 seconds as shown in **Fig.5(a)**, **(b)**. However, even the feedback gains were small, the motion converged to the desired one $\boldsymbol{q} \rightarrow \boldsymbol{q_d}$ after 8 second very well. The tip position also converged to the desired one as shown in Fig.6.

Above results showed the effectiveness of the proposed controller.

VI. Conclusion

This paper has proposed passivity-based controllers for periodic motions of multi-joint robots with impact phenomena. The proposed controllers can generate desired motions, which are specified by users of the controllers. To guarantee stability of the controlled systems, we adopted some assumptions of kinematics and dynamics of the robots and designed the desired motions with some conditions. Even the robot has nonlinear dynamics and discrete dynamics of impact phenomena, we could analyze stability using Lyapunov-like functions owing to these assumptions and conditions.

On the other hand, there seems to remain some important future works. Firstly, to apply the proposed framework to resonance-based control method is our important future work, because resonance-based controllers can reduce actuator torque while generating periodic motions. To adaptively estimate the matrix $\boldsymbol{\Phi}$ is also important. To achieve this adaptation seems to be not so difficult, because we can easily obtain the signals of $\dot{\boldsymbol{q}}(t_{si}^+)$ and $\dot{\boldsymbol{q}}(t_{si}^-)$ online. To prove more rigorous stability for the repetitive controller and to extend the proposed controller for walking robots are also our important future works.

References

[1] Y. Shoji, M. Inaba, T. Fukuda: "Stable Positioning Control of Redundant Multi-link Manipulator with Collision Phenomena," *IEEE International Symposium on Intelligent Control*, pp. 49-54, 1991.

[2] J.W. Grizzle, G. Abba, F. Plestan: "Asymptotically Stable Walking for Biped Robots: Analysis via Systems with Impulse Effects," *IEEE Transaction of Automatic Control*, vol. 46, No. 1, pp. 51-64, 2002.

[3] M.W. Spong, J.K. Holm, L. Dongjun, "Passivity-Based Control of Bipedal Locomotion," *IEEE Robotics and Automation Magazine*, Vol. 14, No. 2, pp. 30-40, 2007.

[4] S. Arimoto: Control Theory of Non-Linear Mechanical Systems: A Passivity-Based and Circuit-Theoretic Approach. *Oxford Engineering Science Series*, 1996.

[5] M. Uemura, S. Kawamura: "Resonance-based Motion Control Method for Multi-Joint Robot through Combining Stiffness Adaptation and Iterative Learning Control", *ICRA2009*, pp. 1543-1548, 2009.

[6] M. Uemura, K. Kimura, S. Kawamura: "Generation of Energy Saving Motion for Biped Walking Robot through Resonance-based Control Method", *IROS2009*, pp. 2928-2933, 2009.

[7] M. Uemura, G. Lu, S. Kawamura, S. Ma: "Passive Periodic Motions of Multi-Joint Robots by Stiffness Adaptation and DFC for Energy Saving", *SICE2008*, pp. 2853-2858, 2008.

[8] M. Uemura, S. Kawamura: "Generation of Energy Saving Motion for Biped Walking Robot through Resonance-based Control Method", *SYROCO2009*, pp. 607-612, 2009.

[9] M. Uemura, K. Kanaoka, S. Kawamura: "Power Assist System for Sinusoidal Motion by Passive Element and Impedance Control", *ICRA2006*, pp. 3935-3940, 2006.

[10] E. R. Westervelt, J. W. Grizzle, C. Chevallereau, J. H. Choi, B. Morris: Feedback Control of Dynamic Bipedal Robot Locomotion. *CRC Press*, 2007.

[11] S. Nakada, T. Naniwa: "A Hybrid Controller of Adaptive and Learning Control for Geometrically Constrained Robot Manipulators ", *IROS 2006*, pp. 4515-4520, 2006.

[12] S. Kawamura, J. Jun, K. Kanaoka, H. Ichii: "A Cascaded Feedback Control Scheme for Trajectory Tracking of Robot Manipulator Systems with Actuator Dynamics", *IROS 2006*, pp. 1504-1509, 2006.